Science of the Total Environment 815 (2022) 152840

Contents lists available at ScienceDirect

Science of the Total Environment

journal homepage: www.elsevier.com/locate/scitotenv

Volatiles and hormones mediated root-knot nematode induced wheat defense response to foliar herbivore aphid

Jin-Hua Shi [1], Hao Liu [1], The Cuong Pham, Xin-Jun Hu, Le Liu, Chao Wang, Caroline Ngichop Foba, Shu-Bo Wang, Man-Qun Wang *

College of Plant Science and Technology, Huazhong Agricultural University, Wuhan 430070, China

HIGHLIGHTS

- Wheat combines tolerance and resistance strategies to cope with multiple attackers.
- Nematode damage has an inhibitory effect on aphid.
- Wheat defense is largely driven by root-knot nematode density and infection time.
- Plant applies various defenses as nematode damages increases.

GRAPHICAL ABSTRACT

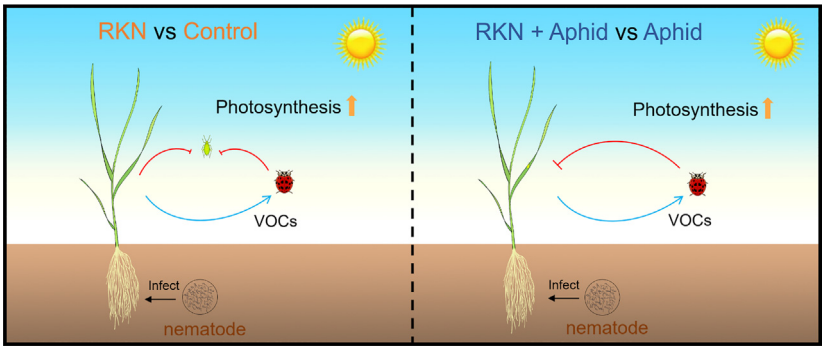

ARTICLE INFO

Article history:
Received 4 March 2021
Received in revised form 26 November 2021
Accepted 28 December 2021
Available online 5 January 2022

Editor: Charlotte Poschenrieder

Keywords:
Aboveground-belowground interactions
Induced systemic resistance
Phytohormones
Volatiles
Plant photosynthesis
Insect behavior

ABSTRACT

Plant root-leaf communication signals are critical for plant defense. Numerous studies show that belowground organisms can alter systemically resistance traits in aboveground parts against herbivores. However, there are limited studies on root-knot nematode-aphid interaction. Moreover, the impact of nematode's initial density and infection time on plant defense is poorly understood. Here we aim to examine the induced defense responses by root-knot nematode *Meloidogyne incognita* against aboveground feeding aphid *Sitobion avenae* in wheat. Further, we investigated the influence of the nematode infection density as well as the length of infection in these interactions. We tested the direct and indirect defense responses triggered by *M. incognita* against *S. avenae* as well as how the responses affect the preference of *Harmonia axyridis*. Plant volatiles and hormones were determined to explore plant defense mechanisms that mediate aboveground-belowground defense. The photosynthetic rate was tested to examine plant tolerance strategy. We found that, both low and high densities *M. incognita* root infection at 7 days post inoculation (dpi) reduced the feeding of the aphid *S. avenae*. Behavioral assay showed that *H. axyridis* preferred plants co-damaged by both *M. incognita* and *S. avenae* at 7 dpi. *M. incognita* infection induced the changes of jasmonic acid, salicylic acid and volatile content, which mediated plant response to *S. avenae*. Furthermore, photosynthetic rate in wheat increased at 5 dpi under 300 *M. incognita* or 1000 *M. incognita* infection. These results suggest that plant roots induced multiple defense strategies against foliar herbivores as damages increased. Our study provides evidence of a complex dynamic response of wheat aboveground defense against aphids in response to belowground nematode damage on a temporal scale.

Abbreviations: AG, aboveground; BG, belowground; dpi, days post inoculation; EPG, Electrical Penetration Graph; GC–MS, Gas chromatography-mass spectrometry; ISR, induced systemic resistance; JA, jasmonic acid; LC-MS, liquid chromatography-mass spectrometry; PCA, Principal Component Analysis; RKN, Root-knot nematode; SA, salicylic acid; VOCs, volatile organic compounds.

* Corresponding author at: College of Plant Science and Technology, Huazhong Agricultural University, Wuhan 430070, China.
E-mail address: mqwang@mail.hzau.edu.cn (M.-Q. Wang).

[1] These authors contribute equally to this work.

http://dx.doi.org/10.1016/j.scitotenv.2021.152840

1. Introduction

In natural and agricultural ecosystem, plants are attacked by different organisms on aboveground (AG) and belowground (BG) parts simultaneously. Plants have evolved sophisticated strategies including tolerance and resistance which they utilize to protect themselves from attackers (Hakes and Cronin, 2012; Kant et al., 2015; Mitchell et al., 2016; Herve and Erb, 2019). Plants rely on tolerance strategy to compensate for damage by changing the assimilation rate, growth, and resources allocation (Robert et al., 2014; Koch et al., 2016). Resistance is when plants can escape attackers partially or fully, thus minimizing the amount of damage. Plant resistance traits include production of compounds that can cause deterrence, death, or reduce the development of the attacker. Depending on the mode of action, plant defense is divided into direct and indirect defense. Direct defense involves the use epidermal physical structures or internal chemically toxic compounds to block feeding or digestion of attackers (Gorb and Gorb, 2017; Beran et al., 2019; Hussain et al., 2019). Brassicaceae accumulate glucosinolate in roots and shoots after *Anomala cuprea* infested (Tsunoda et al., 2018). Indirect defense is mediated by volatile organic compounds (VOCs) (Paré and Tumlinson, 1999; Turlings and Erb, 2018). Plants emit a wide range of VOCs in response to attack by different insect-herbivores and attract their natural enemies (Clavijo McCormick et al., 2012; Turlings and Erb, 2018). The predator lady beetle *Harmonia axyridis* preferred odors of aphid-infested plants than healthy plants of *Cnidium monnieri* (Cai et al., 2020).

Plant hormones play a vital role in regulating direct and indirect defense response (Verberne et al., 2003; Bernsdorff et al., 2016; Klessig et al., 2018; Yuan et al., 2019). Jasmonic acid (JA) and salicylic acid (SA) are recognized as the main signaling pathways regulating direct and indirect defense (Wasternack and Hause, 2013; Dempsey and Klessig, 2017; Xu et al., 2021). In general, JA pathway is activated against chewing herbivores and necrotrophic pathogens (Wasternack and Hause, 2013; Carvalhais et al., 2017), while SA is triggered by sap-sucking herbivores and biotrophic pathogens (Loake and Grant, 2007; Kastner et al., 2014; Dempsey and Klessig, 2017). However, several evidences showed that hormones pathway trigged is variable, and the relationship between JA and SA can be synergistic or antagonistic, depending on the attacking organism and plant systemin (Mur et al., 2006; Koornneef et al., 2008). Other phytohormones such as ABA, ET, also play a role in mediating defense signals (Zhang et al., 2013; Louis et al., 2015; Verma et al., 2016). These hormones may connect to the JA-SA plant defense signaling and are important in later stages of plant defense response (Anderson et al., 2004; Pieterse et al., 2009; Karssemeijer et al., 2020).

The induction of systemic response in undamaged tissues, can cause induced systemic resistance (ISR), or prime the plant systemically (Karssemeijer et al., 2020). ISR increases the resistance levels of undamaged plant parts. Priming, on the other hand, enhances the induced response to later arriving herbivores or pathogens (Guo and Ge, 2017; Mbaluto et al., 2021). ISR and priming can cause interaction between organisms feeding on different plant parts, such as BG roots and AG leaves. Numerous studies have demonstrated that root attackers influence plant resistance in AG (Wäckers and Bezemer, 2003; Soler et al., 2007b; van Geem et al., 2016; Yang et al., 2019). *Spodoptera littoralis* deposited fewer eggs on the plant infested by root-feeding wireworms (*Agriotes lineatus*) (Anderson et al., 2011). On the other hand, AG pests can affect root attackers (Ankala et al., 2013; Hoysted et al., 2018). *P. brassicae* feeding reduced the survival of *Delia radicum* (Soler et al., 2007a). The effect of BG on AG and AG on BG are driven by defense responses signaling via hormonal pathways. Root-knot nematode (RKN) *Meloidogyne incognita* triggered the SA pathway and reduce the reproduction of *Macrosiphum euphorbiae* (Mbaluto et al., 2021). *Plutella xylostella* feeding on *Brassica oleracea* leaves cause a slight change in JA pathway and interact with plant defense to root fly larvae (*Delia radicum*) (Karssemeijer et al., 2020). Moreover, AG and BG attack can influence plant indirect defense responses to interact with the enemies of the attacking herbivores (Soler et al., 2007b; Pierre et al., 2011). *A. lineatus* induced AG indirect defense by producing extrafloral nectar (Wäckers and Bezemer, 2003). While the attraction of the parasitoid (*Trybliographa rapae*) towards *Delia radicum* infested plants disappeared when plants were simultaneously infested by *P. brassicae* (Pierre et al., 2011). The outcome of these AG-BG interactions are reported to be influenced by factors such as sequence of attack (Erb et al., 2011), or attacker feeding mode (Kafle et al., 2017; Karssemeijer et al., 2020). However, the factors have not been well considered in the context of the interaction between RNK and AG aphids.

Root-knot nematodes are plant parasites that infect and cause severe crop damage. In agriculture, it is estimated that RKN causes approximately $157 billion annually globally (Abad et al., 2008). RKN spend most of their life cycle inside plant roots. The main stages include egg - juvenile - adult stage (Abad et al., 2008). The infective second-stage juveniles (J2s) invade plant roots and migrate intercellularly to settle in the vascular cylinder. The activity of RKNs stimulates cell enlargement and produce galls on fibrous roots. RKN reprogram plant defense responses including phytohormonal signaling and secondary metabolite (Molinari and Loffredo, 2006; Bhattarai et al., 2008; Bali et al., 2018). At the same time, root infection by RKN can trigger changes in defense status of AG plant tissues and thus affect insect herbivores (Arce et al., 2017; Guo and Ge, 2017).

Aphid is one of the devastating foliar sucking insect pests of plants (Carter et al., 1982). It can damage plants by feeding on phloem sap and transmitting a variety of viruses. Aphid inject saliva into plants during feeding, and triggers JA and/or SA-dependent plant defense pathways (Kusnierczyk et al., 2011; Morkunas et al., 2011; Liu et al., 2020). Besides, plant can change volatile composition and attract the natural enemy of aphids (Cai et al., 2020).

In nature, RKN and aphid are likely to occur on the same plant. Because they have an analogous feeding style, they are likely to trigger similar defense responses (Hol et al., 2013; Mbaluto et al., 2021). In this study, we hypothesize that differences in RKN density and timing affects the performance of aphids and their natural enemies. More in particular, we hypothesize that the interaction between RKN-aphids and natural enemies is reflected in the induced direct and indirect defense responses. We tested these hypotheses using an important crop species wheat (*Triticum aestivum*) (Langridge, 2013; Borisjuk et al., 2019). It is infected by RKN and aphid leading to yield losses of about 15–20% and 47% globally, respectively. RKN exists in the soil and encountered by wheat plant at the beginning, while aphid generally arrive later in the progress of plant growth. Thus, we set up a series of experiments, in which wheat plants were initially infected with RKN (*M. incognita*) and followed with aphid (*Sitobion avenae*) infestations when the RKN was at different infection time points. In our first experiment, we evaluated *S. avenae* performance when feeding on *M. incognita* infected plants compared to controls. In the second experiment, we assessed the preference of *S. avenae*'s natural enemy *H. axyridis* towards *M. incognita* infected plants and undamaged wheat plants, as well as between co-damaged plants by *M. incognita* and *S. avenae* compared to plant infested with *S. avenae* alone. To explore plant defense mechanisms that mediate AG-BG species interaction, hormones content, volatile composition, and photosynthetic rate of undamaged plant, *M. incognita* or *S. avenae* damaged plant, and co-damaged plant were profiled. Our results showed that the RKN *M. incognita* affect the *S. avenae* and its natural enemy performance by modulating hormones and volatile content.

2. Materials and methods

2.1. Plant, nematode, and insect colony

The wheat variety (Huamai 1168, provided by Prof. Xifeng Ren of Huazhong Agricultural University (HZAU)) was used in all experiments.

Nutrient soil (1.0–5.0% N + P_2O_5 + K_2O and ≥20% organic matter content) was placed in round plastic pots (9 cm diameter × 8 cm height). Seeds were cleaned with sterile water. One seed was sown per pot, and allowed to germinate. Plants were grown under greenhouse conditions at 24 ± 2 °C, 60 ± 10% RH, and 16/8 h light/dark photoperiods at HZAU, Wuhan, China. When the plants were 25 days old after sowing, we selected only those that had four fully formed leaves for bioassays.

Root-knot nematode (*M. incognita*) was used as the BG herbivore. *M. incognita* juveniles were provided by Prof. Yanlong Xiao of HZAU and the colony was maintained on tomato plants (*Solanum lycopersicum*). To obtain the J2 stage of *M. incognita*, infected tomato root-knot was ground and held on a petri dish lined with distilled water-moistened filter paper (qualitative filter paper; diameter: 9 cm; Whatman, China) under room temperature. After 3 days, the filter paper was taken out and rinsed with distilled water. The collected solution was viewed under a 40× optical microscope to count J2 *M. incognita*.

Aphid (*S. avenae*) was used as the AG herbivore. The colony was provided by Prof. Yong Liu of Shandong Agricultural University and maintained on wheat plant var. Luyuan 502 (a sensitive strain for colonizing *S. avenae*). Ladybird adult (*H. axyridis*) was used as natural enemy of *S. avenae*. The ladybird adult was purchased from Zhongke Baiyun Green Bio-Technology Co. Ltd. (Beijing, China). The aphid colony was maintained at 22 °C growth chamber, while the ladybird was maintained at 24 °C growth chambers.

2.2. Nematode inoculation and aphid infestation

Plant infection with herbivores was designed to mimic the natural sequences of events. Because plant roots develop before the leaves, it is likely that nematodes in the soil infect roots before AG herbivores attack the leaves. In all our experiments, the plants that were assigned for *M. incognita* inoculation were divided into two groups. One group received 300 J2/mL (defined as low density) and the other group received 1000 J2/mL (defined as high density). The suspension was diluted to a concentration of about 300 or 1000 *M. incognita*/mL under the microscope. Sample (1 mL) of *M. incognita* solution was inoculated into the soil around the root of wheat plant. Plant without nematode was used as control. Three-time points (3 dpi, 5 dpi, and 7 dpi) were established to mimic the stage of *M. incognita* from invasion to establishment. Plants assigned for AG herbivores were infested with 20 *S. avenae* adults at each time point. Plants were covered by PVC tube (height: 35 cm; diameter: 10 cm) and *S. avenae* fed freely on plant leaves. All *S. avenae* were removed from wheat plant after 24 h. At each of the *M. incognita* infection time points, we established four treatments including (1) control plant (healthy plant); (2) only *M. incognita*-infected plant; (3) only *S. avenae*-damaged plant and (4) simultaneous *M. incognita* and *S. avenae*-damaged plant. Sections of leaf from the damaged or undamaged plants were excised, immediately frozen in liquid nitrogen, and stored at −80 °C until extraction.

2.3. Assessment of the feeding behavior of Sitobion avenae

The feeding behavior of apterous adult *S. avenae* on *M. incognita* infected plant (3 dpi, 5 dpi, or 7 dpi) was recorded using a Giga-4 DC Electrical Penetration Graph (EPG, Wageningen Agricultural University, Wageningen, Netherlands) (Sun et al., 2016). Briefly, a conductive silver glue was used to stick a gold wire (long: 3-cm; diameter: 18.5 mm) to the dorsum of *S. avenae* and placed on the wheat plant. After plant and insect were connected, 5 Vs voltage was added. Feeding waveforms were recorded by Style^{+b} software (Wageningen, The Netherlands) for 12 h at 24 ± 1 °C and 60 ± 10% RH in a Faraday cage. After 50× magnification, five typical waveforms were identified and categorized as previously described (Will et al., 2007; Chen et al., 2018; Chen et al., 2020).

2.4. Assessment of behavior of Harmonia axyridis to herbivore-induced plant volatiles

We tested the response of *H. axyridis* to odors emitted from plants damaged by *S. avenae*, *M. incognita*, or both, using Y-tube olfactometer (arm length: 18 cm and internal diameter: 1.5 cm). The Y-tube was set inside a box to avoid visual cues to the insect (Shi et al., 2019). Each arm of the Y-tube was connected to the odor source (control and treatment) using Teflon tubes and the tested insect was individually released in the main arm. Normal air was filtered through activated charcoal and pumped at a rate of 200 mL/min using battery powered pump (Sensen, Zhejiang, China). A 60 W incandescent lamp bulb was hung above the Y-tube to provide illumination. Every *H. axyridis* adult was given 5 min to make a choice. To avoid positional bias, the Y-tube was switched sides after running test for three insects. Data were recorded from 30 replicates per treatment.

2.5. Extraction and analysis of the phytohormones jasmonic acid and salicylic acid

Ground leaf samples (50 mg each) were extracted by 500 μL extraction solvent (2-propanol/H_2O/concentrated HCl = 2:1:0.002, v/v/v) in a thermostatic mixer (MTC-100, Guangzhou, China) for 30 min at 100 rpm as previously described (Pan et al., 2010). 10 μL Dihydrojasmonic acid (5 μg/mL) and 10 μL D4-Salicylic acid (5 μg/mL) were added as the internal standard of JA and SA, respectively. Dichloromethane (1 mL) was added to the samples and homogenized again. After centrifuging at 13,000 g and at 4 °C for 5 min, the bottom phase was transferred into 2 mL Agilent bottles. Samples were dried by a nitrogen evaporator and dissolved by 100 μL of methanol.

Liquid chromatography-coupled mass spectrometry (LC-MS) system (Xevo G2-XS Qtof) was used to determine JA and SA levels. The relative amount of JA and SA was calculated from the ratio of the endogenous hormone peak and the known internal standard. For each treatment, at least three replicates were analyzed.

2.6. Collection and analysis of volatiles

Plant volatile compounds emitted during herbivory by nematodes and aphids, and control plants were collected using a closed-loop dynamic headspace collection system as described by Sun et al. (Sun et al., 2016). The air was purified by (1) Charcoal (activated carbon, 6 to 14 mesh, Fisher Scientific), (2) 5 A molecular sieves (beads, 8 to 12 mesh, Sigma-Fluka), and (3) silica gel Rubin (drying agent free of metal salts, silica gel, Sigma-Fluka), and pumped at 500 mL/min into a glass jar containing each plant treatment (control plant, *M. incognita*-infected plant, *S. avenae*-damaged plant, or simultaneous *M. incognita* and *S. avenae*-damaged plant). The VOCs were collected for 6 h under light and eluted from Super-Q traps using 1 mL of n-hexane. A 10 μL solution of nonyl acetate (0.1 mg/mL, Sigma-Aldrich, St. Louis, MO, USA) was added to each sample as an internal standard.

The collected volatiles were analyzed using gas chromatography–mass spectrometry device (GC–MS, Agilent Technologies QP-2010, Shimadzu, Shiga, Japan), equipped with an HP-5 MS fused-silica column (30 m × 0.25 mm × 0.25 μm, Agilent Technologies, Palo Alto, CA, USA, http://www.agilent.com). Helium was used as the carrier gas with a flow rate of 1 mL min^{-1}. The initial temperature of the oven was 40 °C and held for 1 min, and then at 8 °C min^{-1} to 300 °C and held for 5 min. The mass spectrometer of the GC–MS instrument was operated in an electron-impact mode (EI) at 70 eV, with a scan range of m/z 40–450. The transfer line temperature was set at 220 °C and ion-source temperature at 200 °C. The volatile compounds were identified by comparing their GC retention indices and MS spectra with those from the NIST11 library (http://nistmassspeclibrary.com). Each treatment was replicated at least four times.

2.7. Assessment of photosynthetic rate of wheat plant

Li-6400XT portable photosynthesis system (Li-Cor, Lincoln, NE, USA) was used to determine the net photosynthetic rate of wheat plant (Molero and Reynolds, 2020). Wheat leaf (the second leaf) was placed into the leaf chamber. CO_2 gas bomb was used to inject CO_2 into the system. The airflow was set at a speed of 500 μmol/s. The temperature of the leaf chamber was 24 °C, with a CO_2 concentration of 400 μmol/mol, light source intensity of 1500 mol/m^2/s, and a water vapor pressure difference of approximately 1.2 kPa. Data collection was performed in 9:00–12:00 daytime in the greenhouse. Leaf area placed into the chamber was determined to calculate plant photosynthetic capacity of per unit area. Each treatment was replicated at least four times.

2.8. Data analyses

All data were analyzed in R (4.0.3) (Team, 2013). Y tube data were analyzed by Chi-square test. One or two ANOVA was used to analyze data from aphid feeding performance, phytohormone concentration, volatile content, and photosynthesis rate among different treatments. In the model of ANOVA, we included nematode density and infection time as variable factor and waveform duration, waveform frequency, phytohormone concentration, volatile content, or photosynthesis rate as explanatory factor. Tukey's HSD was used as post hoc analysis to detect the significant differences at $P < 0.05$. Principal component analysis (PCA) was performed on the volatile data and PerMANOVA based on Bray-Curtis was used to comparing the contribution of factors (nematode density and infection time).

3. Results

3.1. Impact of Meloidogyne incognita on the feeding behavior of Sitobion avenae

We assessed the impact of *M. incognita* infection density (300-low and 1000-high) and different time points (3,5,7 dpi) on the feeding behavior *S. avenae* (Fig. 1). At 3 and 5 dpi, we found that *M. incognita* root infection only affected the E1 waveform. The results showed that both low and high infection densities were not different from control plants. However, there was a significant decrease in E1 in high density compared to low density (Fig. 1a, b; Table S1). At 7 dpi, the results showed that the influence of *M. incognita* root infection on E1 waveform duration disappeared. The low *M. incognita* density infection significantly increased np and C waveform duration but decreased E2 waveform duration compared to control plants. The high *M. incognita* density infection significantly increased C waveform duration but decreased G waveform compared to control plants. There was a significant decrease in np and G waveform duration but an increase in E2 waveform duration in high density compared to low density (Fig. 1c; Table S1).

M. incognita root infection did not change waveforms frequency at 3 dpi and 5 dpi (Fig. 2a, b; Table S2). At 7 dpi, the low *M. incognita* density infection increased the frequency occurrence of np waveform compared to high density and control plants, while there was no significant difference of np waveform frequency between control and high *M. incognita* density infected plants. Compared with control plants, low density infection increased C waveform frequency but showed no significant difference in high density infected plants (Fig. 2c; Table S2).

Two-way ANOVA showed that the density of *M. incognita* significantly affected the duration of np, C, E1, and E2 and the frequency occurrence of np and C waveforms, while infection time significantly affected the duration of np and E1 waveforms (Table S3, S4). Besides, the density of nematodes versus infection time interaction affected the duration of np and frequency of C waveforms.

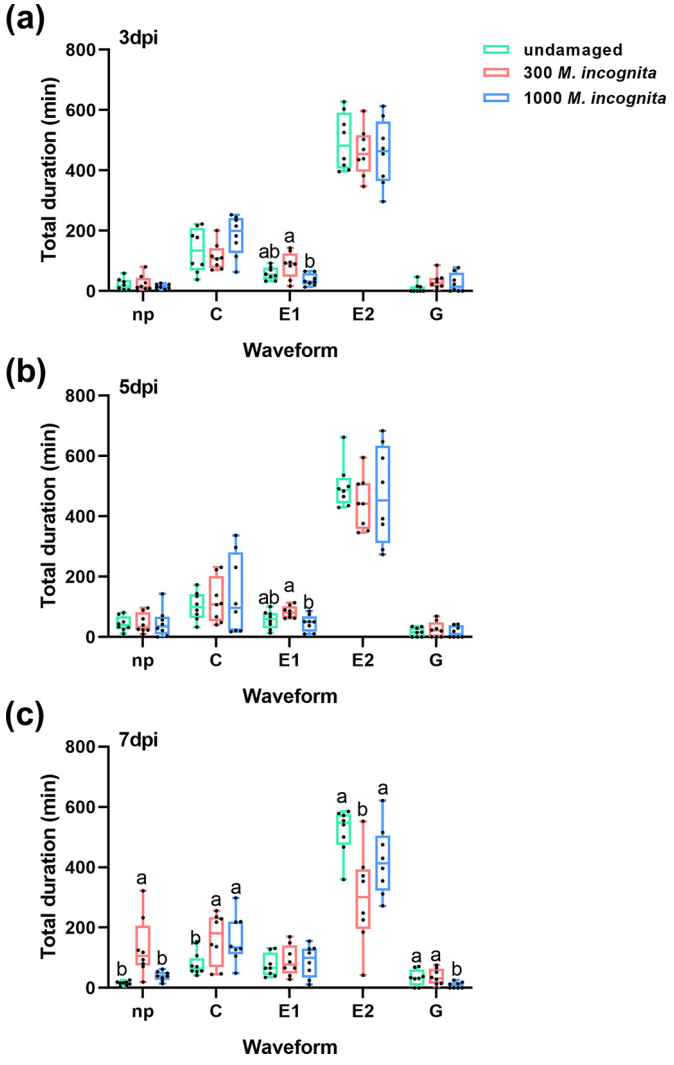

Fig. 1. EPG recordings of the aphid *Sitobion avenae* feeding duration in wheat plants infected by 300 or 1000 *Meloidogyne incognita* against undamaged plant at different time points (3 dpi, 5 dpi, or 7 dpi). Dpi: days post inoculation. Different letters indicate significant differences ($P < 0.05$) among treatments ($n = 8$).

3.2. Impact of Meloidogyne incognita on the preference of Sitobion avenae natural enemy Harmonia axyridis

We tested the preferences of *H. axyridis* to *M. incognita* infected plant or *M. incognita* and *S. avenae* co-damaged plant (Fig. 3; Table S5). The results showed that no obvious differences occurred at 3 or 5 d *M. incognita* infection (Fig. 3a, b; Table S5). However, after 7 dpi, *H. axyridis* significantly preferred high *M. incognita* density infected plants over undamaged plants, while there were no obvious differences under low *M. incognita* density (Fig. 3c; Table S5). After *S. avenae* damage, *H. axyridis* significantly preferred *M. incognita* and *S. avenae* co-damaged plant than *S. avenae* damaged plant after 7 dpi of *M. incognita* at both densities (Fig. 3c; Table S5).

3.3. Jasmonic acid and salicylic acid regulate wheat defense to Sitobion avenae

We first analyzed for changes in JA and SA concentrations at different time points and infection densities. We found that *M. incognita* root infection in low density increased the JA levels at 3 dpi but no effect at 5 and 7 dpi compared to control (Fig. 4 a, e, i; Table S6). However, high density *M. incognita* root infection increased the JA levels at 3 or 7 dpi compared

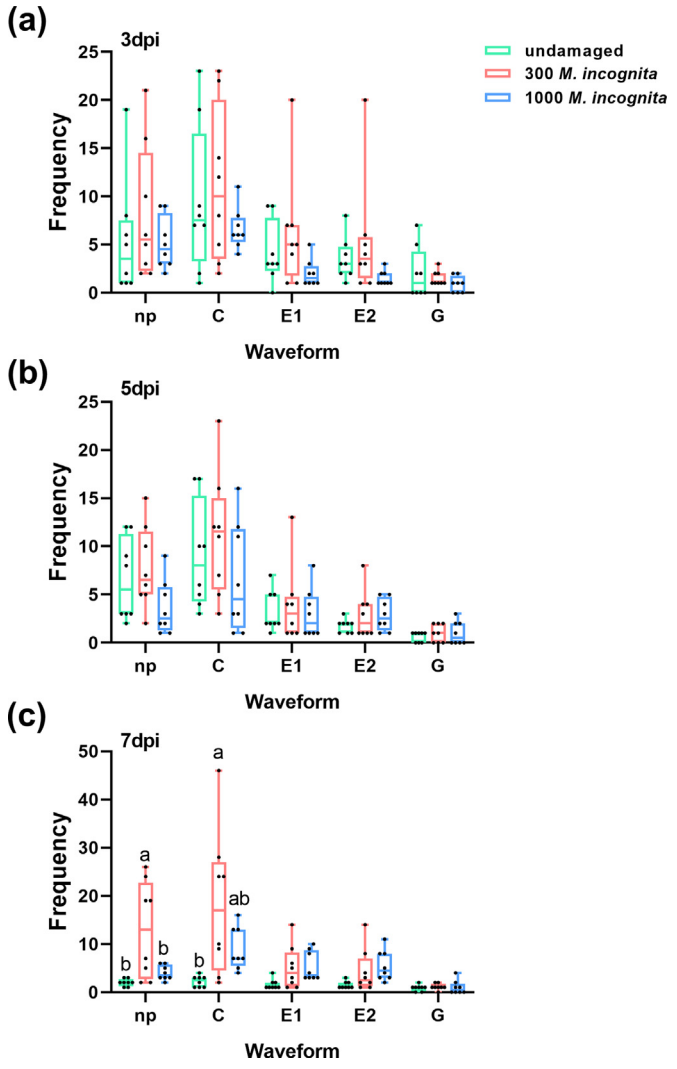

Fig. 2. EPG recordings of the aphid *S. avenae* feeding frequency in wheat plants infected by 300 or 1000 *M. incognita* against undamaged plant at different time points (3 dpi, 5 dpi, or 7 dpi). Dpi: days post inoculation. Different letters indicate significant differences ($P < 0.05$) among treatments ($n = 8$).

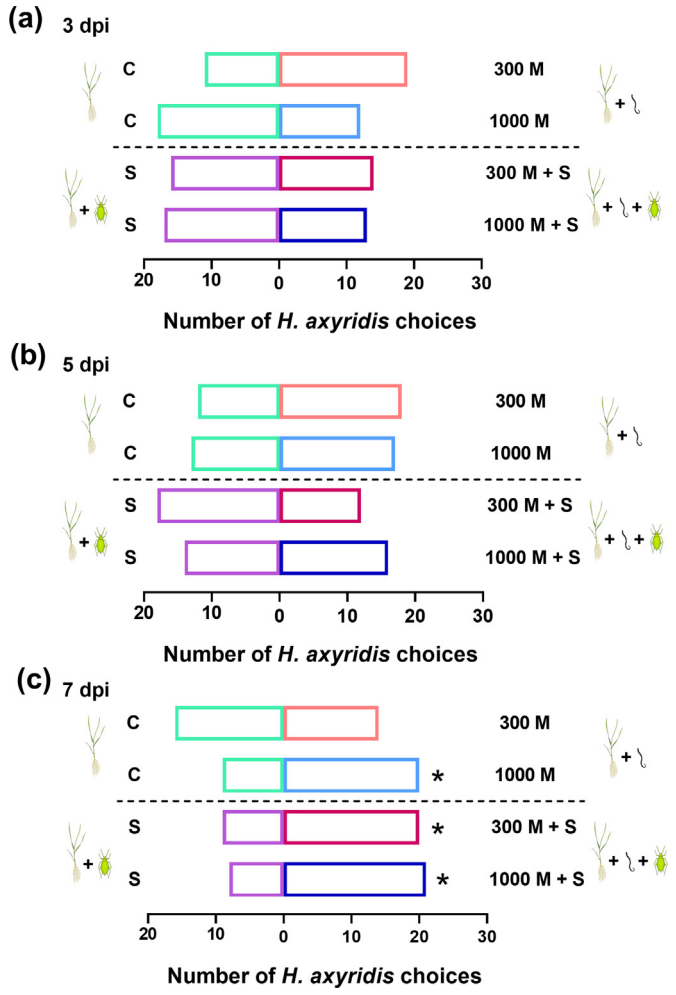

Fig. 3. Preference behavior of ladybird beetle *Harmonia axyridis* in Y-tube under 300 or 1000 *M. incognita* damage at different time points (3 dpi, 5 dpi, or 7 dpi). C: Control plant; M: *M. incognita* infected plant; S: *S. avenae* damaged plant; M + S: simultaneous *M. incognita* and *S. avenae*-damaged plant. Dpi: days post inoculation. * $P < 0.05$ ($n = 30$).

to control (Fig. 4b, f, j; Table S6). *M. incognita* root infection in low density or high density did not alter SA levels at all the three time points compared to control (Fig. 4c, d, g, h, k, l; Table S6).

Compared to control plant, *S. avenae* damage showed no obvious influence on JA levels but significantly increased SA levels at most time points (Fig. 4; Table S6). When *M. incognita* and *S. avenae* co-damaged, JA levels showed no significant change compared to *S. avenae* damaged plant at all the three time points and the two *M. incognita* densities (Fig. 4a, b, e, f, i, j; Table S6). While SA level was largely dependent on the *M. incognita* infection density. In the low *M. incognita* density, *M. incognita* and *S. avenae* co-damaged decreased SA level at 3 dpi and 5 dpi compared to *S. avenae* damaged plant, while no significant difference occurred at 7 dpi (Fig. 4c, g, k; Table S6). However, in the high density *M. incognita* and *S. avenae* co-damaged plant, SA level increased at 3 dpi but no effect at 5 and 7 dpi compared to *S. avenae* damaged plant (Fig. 4d, h, i; Table S6). Two-way ANOVA showed that nematode density significantly affected both JA and SA content, while infection time significantly affected only SA content (Table S7).

3.4. Meloidogyne incognita induced VOCs in wheat plant

In total, nine volatile components were extracted and identified, including several alkanes (tetradecane, pentadecane, hexadecane), alkene (tetradecene), alcohol (2-ethyl-hexanol), aldehydes (nonanal, decanal), and ketones (acetophenone, 2-bornanone) (Table S8, S9). PCA showed that volatile composition was different after low *M. incognita* density infection at 3 dpi, 5 dpi, and 7 dpi (Fig. 5a-c). According to the contributions of volatiles to the first two principal components, 2-ethyl-hexanol, decanal, tetradecane, pentadecane and hexadecane played important roles at 3 dpi (Fig. 5d). Nonanal, tetradecene, tetradecane, pentadecane and hexadecane play important roles at 5 dpi (Fig. 5e). 2-ethyl-hexanol, nonanal, decanal, and pentadecane played important roles at 7 dpi (Fig. 5f).

The volatile composition was also different after high *M. incognita* density infection at 3 dpi, 5 dpi, and 7 dpi (Fig. 6a-c). According to the contributions of volatiles to the first two principal components, decanal, tetradecane, pentadecane and hexadecane played important roles at 3 dpi (Fig. 6d). 2-Ethyl-hexanol, acetophenone, nonanal, 2-bornanone, tetradecane, and hexadecane played important roles at 5 dpi (Fig. 6e). 2-Ethyl-hexanol, nonanal, 2-bornanone, decanal, tetradecane, pentadecane, hexadecane played important roles at 7 dpi (Fig. 6f).

The content of prominent volatiles was compared across treatment. After low *M. incognita* density infection, the content of decanal was highest in *S. avenae* infested plant, tetradecene and hexadecane were increased in *S. avenae* damaged plants and *M. incognita* and *S. avenae* co-

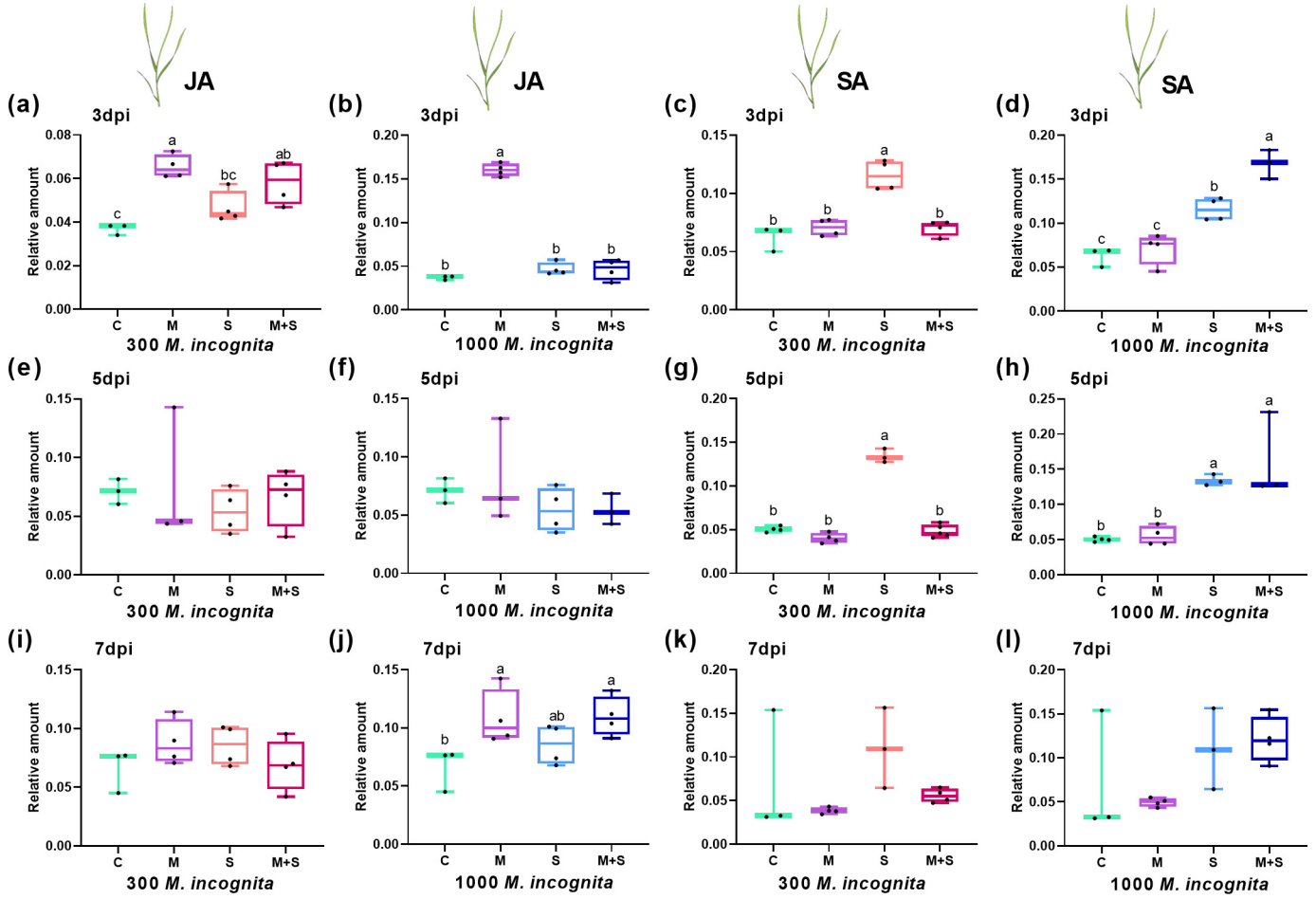

Fig. 4. Plant phytohormones produced after 300 or 1000 *M. incognita* damage against undamaged wheat plant at different time points (3 dpi, 5 dpi, or 7 dpi). C: Control plant; M: *M. incognita* infected plant; S: *S. avenae* damaged plant; M + S: simultaneous *M. incognita* and *S. avenae*-damaged plant. Dpi: days post inoculation. Different letters indicate significant differences ($P < 0.05$) among treatments ($n = 3$–4).

damaged plants at 3 dpi (Fig. 7a; Table S10). The content of nonanal, tetradecane, pentadecane and hexadecane was highest in *M. incognita* and *S. avenae* co-damaged plants at 5 dpi (Fig. 7b; Table S10). The content of nonanal, decanal and pentadecane were highest in *S. avenae* damaged plants at 7 dpi (Fig. 7c; Table S10). After high *M. incognita* density infection, the content of tetradecane and hexadecane was highest in *S. avenae* damaged plants at 3 dpi (Fig. 7d; Table S11). The content of 2-bornanone and hexadecane was highest in *S. avenae* damaged plants at 5 dpi (Fig. 7e; Table S11). The content of nonanal and pentadecane was highest in *S. avenae* damaged plants (Fig. 7f; Table S11). PerMANOVA showed that *M. incognita* density significantly affected volatile composition, while infection time showed no obvious effect on wheat volatile (Table S12).

3.5. Meloidogyne incognita induced photosynthesis compensation of wheat plant

The plant photosynthesis was analyzed at different time points and infection densities. Our results showed that *M. incognita* root infection in low density did not significantly affect plant photosynthesis at 3 dpi compared to control (Fig. 8a; Table S13). While plant photosynthesis increased at 5 dpi and decreased at 7 dpi (Fig. 8c, e; Table S13). When plant infected by high *M. incognita* density, plant photosynthesis was increased at all the three time points compared to control (Fig. 8b, d, f; Table S13). Plant photosynthesis was also significantly increased in *S. avenae* damaged plants compared to undamaged plant. When *S. avenae* and low *M. incognita* density co-occurred, photosynthesis significantly increased at 5 dpi but decrease at 7 dpi compared to *S. avenae* damage (Fig. 8a, c, e; Table S13). Photosynthesis in *S. avenae* and high *M. incognita* density co-occurred plant was decreased at 3 dpi but showed no significant difference at 5 or 7 dpi compared to *S. avenae* damaged plant (Fig. 8b, d, f; Table S13). Two-way ANOVA showed that *M. incognita* density, infection time, and interaction between them significantly affected photosynthesis (Table S14).

4. Discussion

Plants are constantly exposed to AG and BG attackers, and have evolved complex defense systems composed of multiple layers to cope with attackers (Wäckers and Bezemer, 2003; Soler et al., 2007b). This study investigated the influence of BG RKN to plant defense against AG aphid. Our results showed that, with increasing infection density and time, RKN triggered ISR blocked AG aphid feeding and recruited the natural enemy of aphid. Besides, RKN infection changed hormones level and increased photosynthesis of plant.

The feeding behavior of *S. avenae* on 300 or 1000 *M. incognita* infected plant was determined by EPG technology. EPG technology can record duration and frequency of stylet tip's location and reflect the plant defense to insects (Will et al., 2007; Chen et al., 2018; Chen et al., 2020). Various studies showed that plant parasitic nematode root infection can increase plant defense to AG herbivores (Hol et al.,

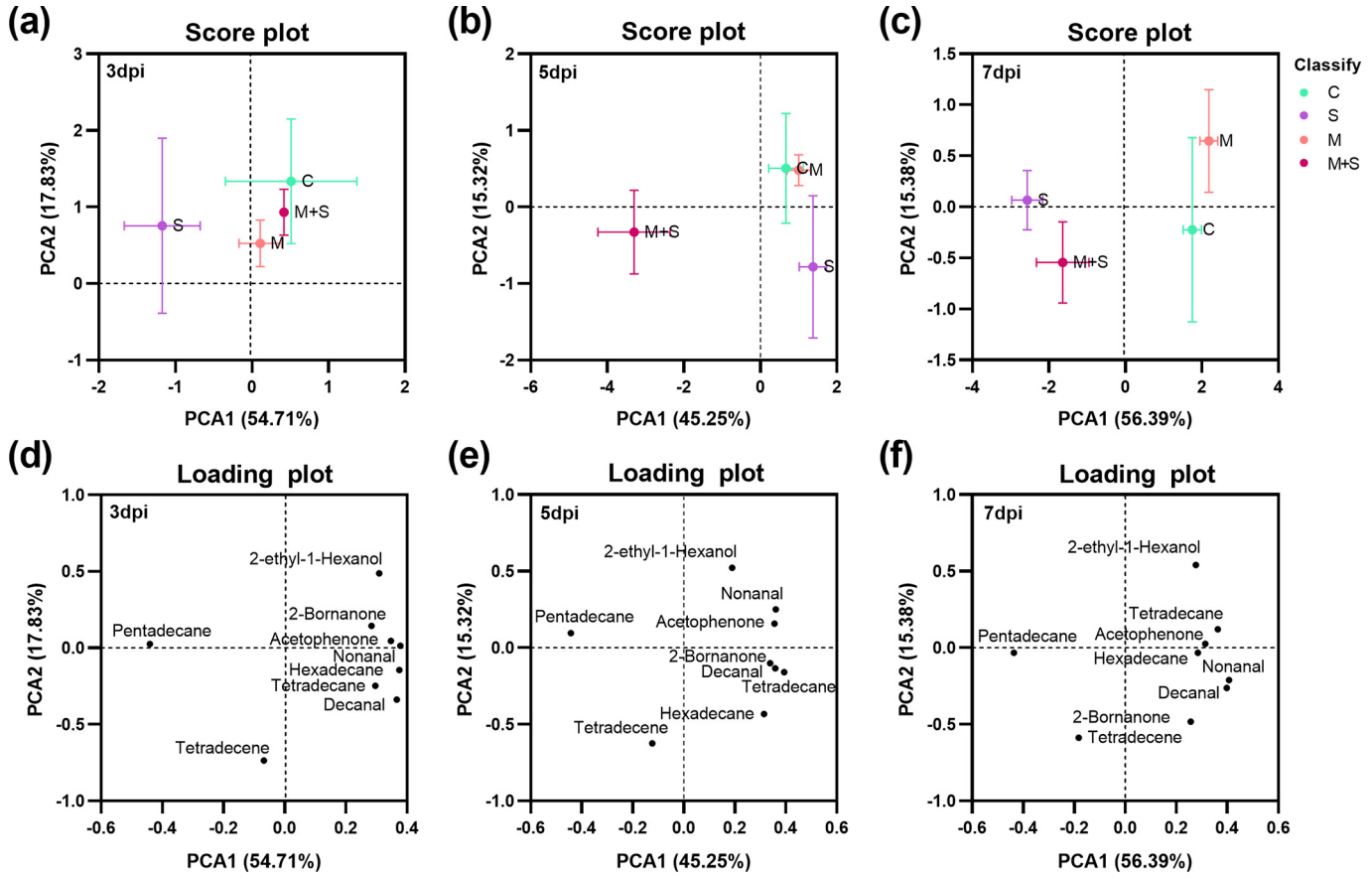

Fig. 5. Wheat plant volatiles from control plant, 300 *M. incognita* infected plant, *S. avenae* damaged plant, 300 *M. incognita* and *S. avenae* co-damaged plant at different time points (3 dpi, 5 dpi, or 7 dpi). (a–c) Score scatter plot of samples according to the first two principal components at different time points. (d–f) Loading plot of wheat plant volatiles at different time points. C: Control plant; M: *M. incognita* infected plant; S: *S. avenae* damaged plant; M + S: simultaneous *M. incognita* and *S. avenae*-damaged plant. Dpi: days post inoculation. Different letters indicate significant differences ($P < 0.05$) among treatments ($n = 4–6$).

2013; Arce et al., 2017; Guo and Ge, 2017). Similar to other studies, our EPG results showed that *M. incognita* infection has an adverse effect on *S. avenae* feeding, especially at 7 dpi. Interestingly, 7 d after low *M. incognita* density damage on plant occurred, the feeding resistance to *S. avenae* was observed in the plant epidermis (duration of np waveform), parenchyma cells (duration of C waveform), and phloem (duration of E2 waveform). Feeding resistance to *S. avenae* at 7 dpi in high density *M. incognita*-infected plant, mainly occurred in mesophyll cells (duration of C waveform). This may likely be attributed to the production of certain plant external physical structural changes and internal anti-insect secondary metabolites triggered by *M. incognita* infection that hindered *S. avenae* feeding. Additionally, *M. incognita*-induced plant direct defense against *S. avenae* was affected by both infection density and time. Future research needs to evaluate the (such as wax microstructural variation) in plant epidermis by scanning electron microscopy, as well as determine the secondary metabolites induced by *M. incognita*. Such studies will help develop aphid-resistant wheat strains by gene editing.

It is widely reported that a complex relationship exists between hormonal pathways in plant defense, including coordination, prioritization, and cross-talk (Schweiger et al., 2014; Wei et al., 2014; Ku et al., 2018; Jang et al., 2020). Our studies showed that hormone signaling pathways mediated by *M. incognita* regulate defense responses to *S. avenae*. After *M. incognita* infection, JA amount was increased while SA showed no significant changes. In addition to the fact that plant had direct resistance to *S. avenae* feeding, JA may mediate wheat defense against *S. avenae*. Previous studies also showed JA mediate plant defense to both nematode and aphid (Bhattarai et al., 2008; Kusnierczyk et al., 2011; Morkunas et al., 2011; Zhao et al., 2015; Bali et al., 2018). However, high density increased JA level at 7 dpi while low density showed no effect on JA level. Plant defense to herbivores damage is density dependence (Underwood, 2000; Cai et al., 2014; Desurmont et al., 2018). The interactions of the hormone pathway trigger appropriate defense responses in plants (Morkunas et al., 2011; Schweiger et al., 2014; Wei et al., 2014; Jang et al., 2020). Thus, a comparative analysis of the link between gene expression of hormone signals and induced downstream defense metabolites is required to confirm this hypothesis in different plant-herbivores systems.

Insect damage on plants results in the emission of volatile organic compounds. These VOCs are indirect plant defenses that recruit the natural enemies to the attacking herbivore (Bruce et al., 2005; Duan et al., 2019). Root attacking organisms have been reported to trigger the emission of VOC in AG organs (Rasmann and Turlings, 2007; Soler et al., 2007b). Our study showed that high density *M. incognita* induced plant volatile had a strong attraction to *H. axyridis* in wheat plant at 7 dpi. *H. axyridis* also preferred odors from simultaneously 7 dpi with RKN and *S. avenae* fed wheat plant. This can be linked to plant volatile profiles which showed that nematode-mediated indirect resistance in wheat plant plays an important role in defense against *S. avenae*. However, *S. avenae* induced more volatiles at 7 dpi compared to *M. incognita* and *S. avenae* co-damaged plant. Although the plant volatile contents

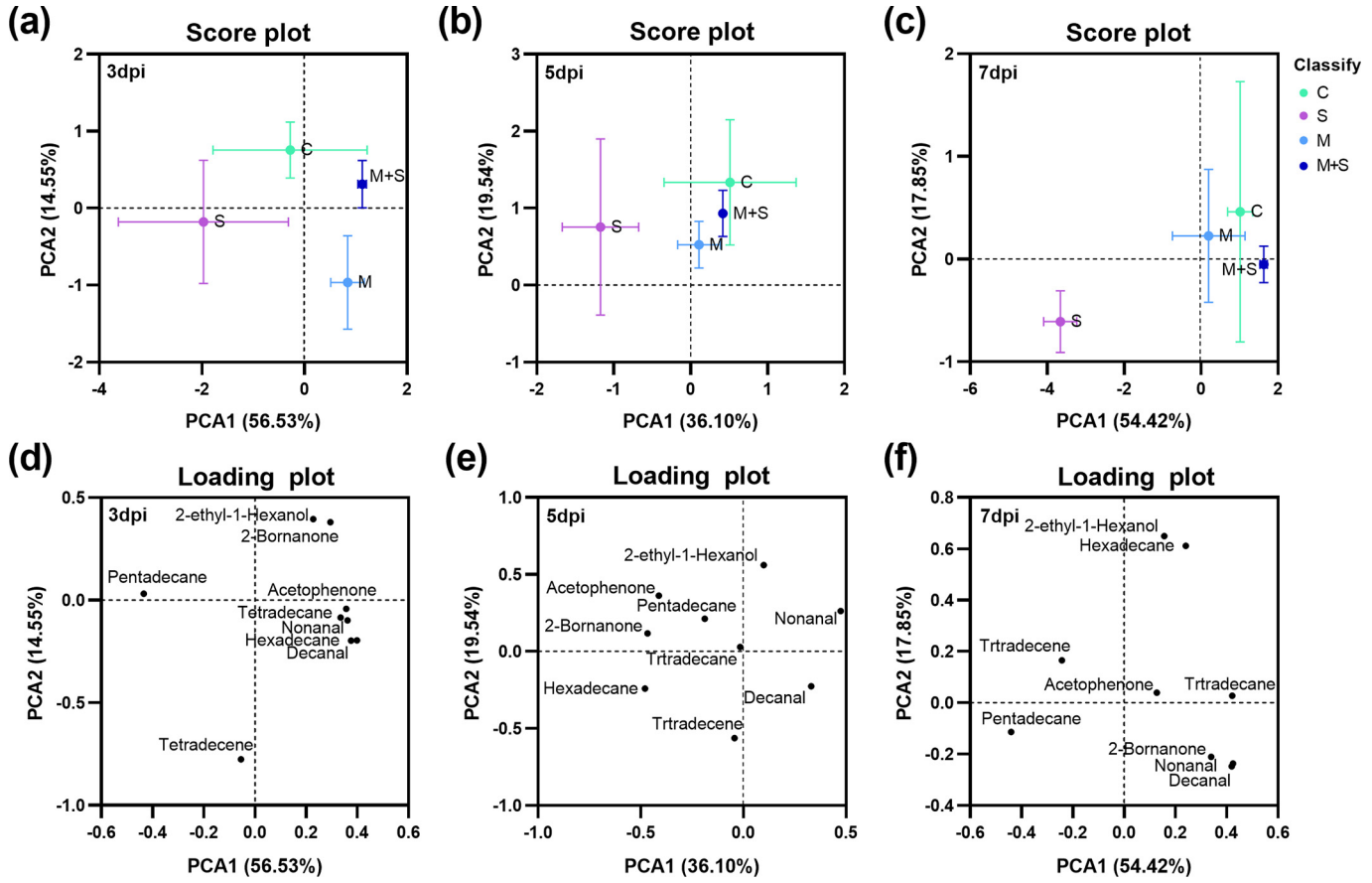

Fig. 6. Wheat plant volatiles from control plant, 1000 *M. incognita* infected plant, *S. avenae* damaged plant, 1000 *M. incognita* and *S. avenae* co-damaged plant at different time points (3 dpi, 5 dpi, or 7 dpi). (a–c) Score scatter plot of samples according to the first two principal components at different time points. (d–f) Loading plot of wheat plant volatiles at different time points. (g–i) Prominent volatiles contribute to the first two principal components. C: Control plant; M: *M. incognita* infected plant; S: *S. avenae* damaged plant; M + S: simultaneous *M. incognita* and *S. avenae*-damaged plant. Dpi: days post inoculation. Different letters indicate significant differences ($P < 0.05$) among treatments ($n = 4$–6).

were not stable in this study, herbivores evolve sophisticated olfactory systems and show a positive response to proportionally volatile blends. To further find the specific volatile in responsible to attracting *H. axyridis*, there is a need for in-depth studies using GC-EAD methods to test *H. axyridis* response to volatile compounds in different concentrations.

Plant can increase photosynthetic ability and adopt a tolerance strategy under biotic pressure (Johnson et al., 2012; Karley et al., 2016; Nalam et al., 2019). Wheat plant displayed an increase in photosynthetic ability following *M. incognita* damage, especially after high density *M. incognita* damage. *M. incognita* damage also increased photosynthetic ability when *S. avenae* damage occurred. Our findings showed that plant may allocate energy to tolerance under *M. incognita* infection. Bali et al. applied JA to induced tolerance on RKNs infected plants through altered photosynthesis (Bali et al., 2018). Plant can balance growth and defense to better adapt to the environment (Huot et al., 2014; Robert et al., 2014; Zust and Agrawal, 2017). Therefore, trade-off between plant growth and defense signals induced by nematode need to be further tested.

In conclusion, wheat defense to *M. incognita* can transmit from root to shoot, which block *S. avenae* feeding and recruit *H. axyridis*. This effect was modulated by hormones and volatile content and influenced by *M. incognita* infection density and time. Our results provide basis for future studies underlying the ecological implications behind plant interacting with BG *M. incognita* to predict AG *S. avenae* performance. Further studies need to elucidate the pathway involved in tolerance and resistance cross-talk, and also explore the ecological implications of root-shoot defense response in wheat to the target and other similar pests.

CRediT authorship contribution statement

Jin-Hua Shi: Conceptualization, Investigation, Formal analysis, Data curation, Writing – original draft. **Hao Liu:** Conceptualization, Investigation, Formal analysis, Data curation, Writing – original draft. **The Cuong Pham:** Investigation, Formal analysis, Data curation. **Xin-Jun Hu:** Investigation, Formal analysis, Data curation. **Le Liu:** Investigation, Formal analysis, Data curation. **Chao Wang:** Formal analysis, Data curation. **Caroline Ngichop Foba:** Writing – original draft. **Shu-Bo Wang:** Investigation. **Man-Qun Wang:** Conceptualization, Formal analysis, Data curation, Writing – original draft.

Declaration of competing interest

The authors declare that they have no known competing financial interests or personal relationships that could have appeared to influence the work reported in this paper.

Acknowledgements

We thank the College of Plant Science and Technology Metabolomics Facility, Huazhong Agriculture University for the analysis of the volatile

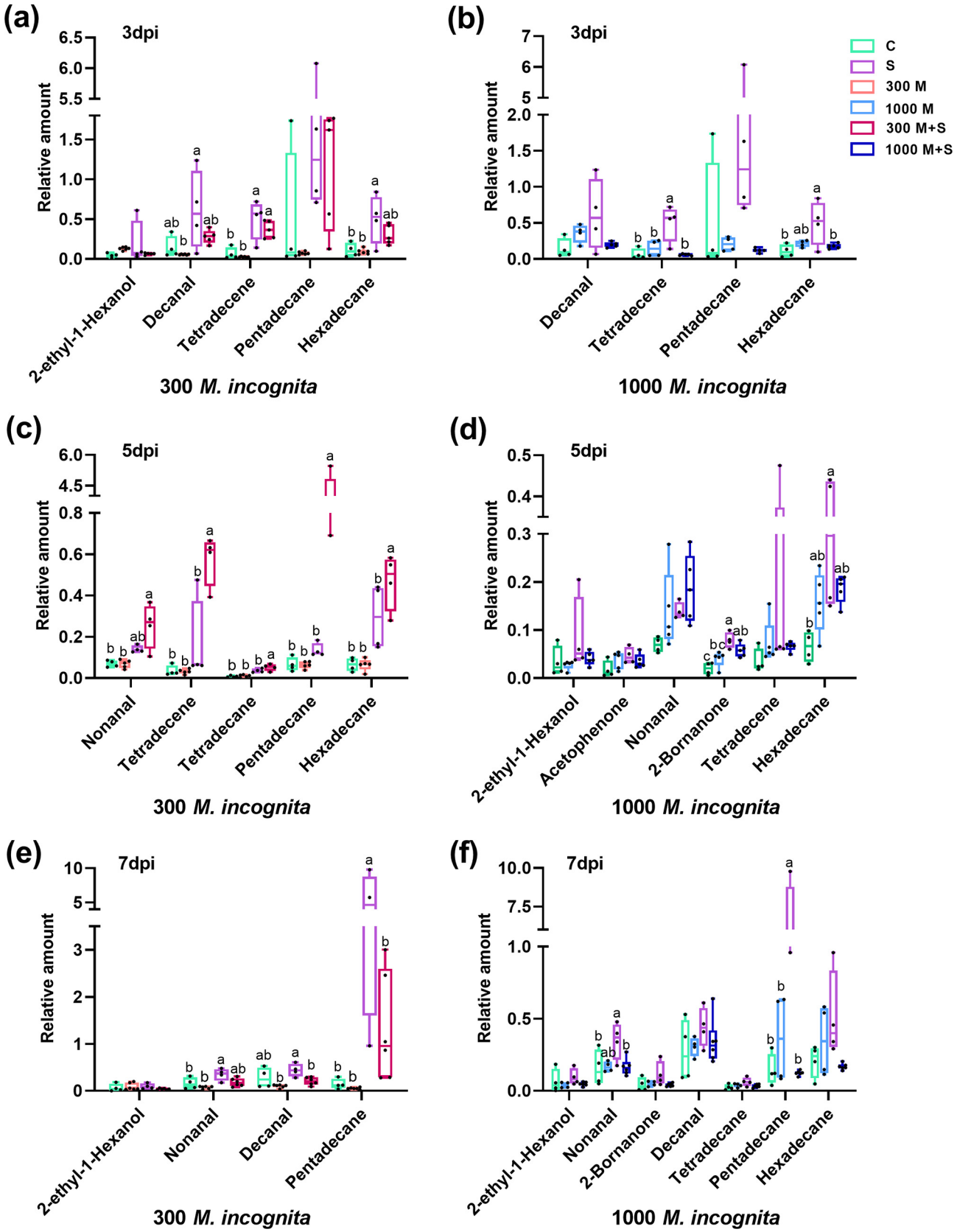

Fig. 7. Prominent volatiles contribute to the first two principal components of PCA. C: Control plant; M: *M. incognita* infected plant; S: *S. avenae* damaged plant; M + S: simultaneous *M. incognita* and *S. avenae*-damaged plant. Dpi: days post inoculation. Different letters indicate significant differences ($P < 0.05$) among treatments ($n = 4$–6).

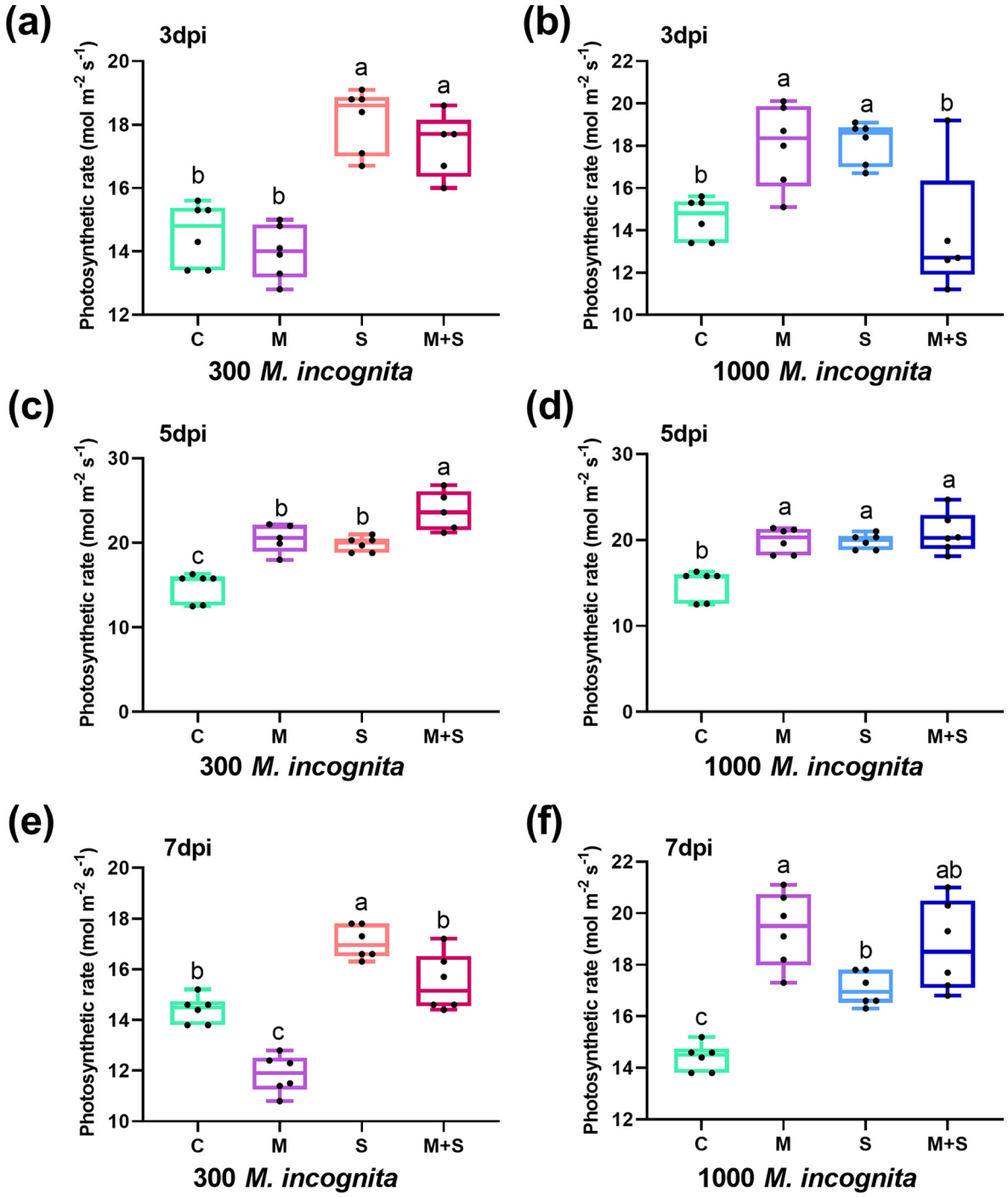

Fig. 8. Plant photosynthetic compensation of wheat plant under 0, 300, or 1000 *M. incognita* damage at different time points (3 dpi, 5 dpi, or 7 dpi). C: Control plant; M: *M. incognita* infected plant; S: *S. avenae* damaged plant; M + S: simultaneous *M. incognita* and *S. avenae*-damaged plant. Dpi: days post inoculation. Different letters indicate significant differences ($P < 0.05$) among treatments ($n = 4$–6).

compounds and phytohormones. This study was supported and funded by the National Key Research and Development Program of China (2017YFE0113900) and Egypt-China Cooperation Program (30369). We thank the editor and reviewers for their constructive comments and suggestions on improving our manuscript.

Appendix A. Supplementary data

Supplementary data to this article can be found online at https://doi.org/10.1016/j.scitotenv.2021.152840.

References

Abad, P., Gouzy, J., Aury, J.M., Castagnone-Sereno, P., Danchin, E.G., Deleury, E., Perfus-Barbeoch, L., Anthouard, V., Artiguenave, F., Blok, V.C., Caillaud, M.C., Coutinho, P.M., Dasilva, C., De Luca, F., Deau, F., Esquibet, M., Flutre, T., Goldstone, J.V., Hamamouch, N., Hewezi, T., Jaillon, O., Jubin, C., Leonetti, P., Magliano, M., Maier, T.R., Markov, G.V., McVeigh, P., Pesole, G., Poulain, J., Robinson-Rechavi, M., Sallet, E., Segurens, B., Steinbach, D., Tytgat, T., Ugarte, E., van Ghelder, C., Veronico, P., Baum, T.J., Blaxter, M., Bleve-Zacheo, T., Davis, E.L., Ewbank, J.J., Favery, B., Grenier, E., Henrissat, B., Jones, J.T., Laudet, V., Maule, A.G., Quesneville, H., Rosso, M.N., Schiex, T., Smant, G., Weissenbach, J., Wincker, P., 2008. Genome sequence of the metazoan plant-parasitic nematode Meloidogyne incognita. Nat. Biotechnol. 26, 909–915.

Anderson, J.P., Badruzsaufari, E., Schenk, P.M., Manners, J.M., Desmond, O.J., Ehlert, C., Maclean, D.J., Ebert, P.R., Kazan, K., 2004. Antagonistic interaction between abscisic acid and jasmonate-ethylene signaling pathways modulates defense gene expression and disease resistance in Arabidopsis. Plant Cell 16, 3460–3479.
Anderson, P., Sadek, M., Wäckers, F.L., 2011. Root herbivory affects oviposition and feeding behavior of a foliar herbivore. Behav. Ecol. 22, 1272–1277.
Ankala, A., Kelley, R.Y., Rowe, D.E., Williams, W.P., Luthe, D.S., 2013. Foliar herbivory triggers local and long distance defense responses in maize. Plant Sci. 199, 103–112.
Arce, C.C., Machado, R.A., Ribas, N.S., Cristaldo, P.F., Ataíde, L.M., Pallini, Â., Carmo, F.M., Freitas, L.G., Lima, E., 2017. Nematode root herbivory in tomato increases leaf defenses and reduces leaf miner oviposition and performance. J. Chem. Ecol. 43, 120–128.
Bali, S., Kaur, P., Sharma, A., Ohri, P., Bhardwaj, R., Alyemeni, M.N., Wijaya, L., Ahmad, P., 2018. Jasmonic acid-induced tolerance to root-knot nematodes in tomato plants through altered photosynthetic and antioxidative defense mechanisms. Protoplasma 255, 471–484.
Beran, F., Kollner, T.G., Gershenzon, J., Tholl, D., 2019. Chemical convergence between plants and insects: biosynthetic origins and functions of common secondary metabolites. New Phytol. 223, 52–67.
Bernsdorff, F., Doring, A.C., Gruner, K., Schuck, S., Brautigam, A., Zeier, J., 2016. Pipecolic acid orchestrates plant systemic acquired resistance and defense priming via salicylic acid-dependent and -independent pathways. Plant Cell 28, 102–129.
Bhattarai, K.K., Xie, Q.G., Mantelin, S., Bishnoi, U., Girke, T., Navarre, D.A., Kaloshian, I., 2008. Tomato susceptibility to root-knot nematodes requires an intact jasmonic acid signaling pathway. Mol. Plant-Microbe Interact. 21, 1205–1214.
Borisjuk, N., Kishchenko, O., Eliby, S., Schramm, C., Anderson, P., Jatayev, S., Kurishbayev, A., Shavrukov, Y., 2019. Genetic Modification for Wheat Improvement: from Transgenesis to Genome Editing. Biomed. Res. Int. 2019, 6216304.
Bruce, T.J., Wadhams, L.J., Woodcock, C.M., 2005. Insect host location: a volatile situation. Trends Plant Sci. 10, 269–274.
Cai, X.-M., Sun, X.-L., Dong, W.-X., Wang, G.-C., Chen, Z.-M., 2014. Herbivore species, infestation time, and herbivore density affect induced volatiles in tea plants. Chemoecology 24, 1–14.
Cai, Z., Ouyang, F., Su, J., Zhang, X., Liu, C., Xiao, Y., Zhang, J., Ge, F., 2020. Attraction of adult Harmonia axyridis to volatiles of the insectary plant Cnidium monnieri. Biol. Control 143, 104189.
Carter, N., Dixon, A.F.G., Rabbinge, R., 1982. Cereal aphid populations: biology, simulation and prediction. Agric. Syst. 11, 184–186.
Carvalhais, L.C., Schenk, P.M., Dennis, P.G., 2017. Jasmonic acid signalling and the plant holobiont. Curr. Opin. Microbiol. 37, 42–47.
Chen, C., Ye, S., Hu, H., Xue, C., Yu, X., 2018. Use of electrical penetration graphs (EPG) and quantitative PCR to evaluate the relationship between feeding behaviour and Pandora neoaphidis infection levels in green peach aphid Myzus persicae. J. Insect Physiol. 104, 9–14.
Chen, Y., Rong, X., Fu, Q., Li, B., Meng, L., 2020. Effects of biochar amendment to soils on stylet penetration activities by aphid Sitobion avenae and planthopper Laodelphax striatellus on their host plants. Pest Manag. Sci. 76, 360–365.
Clavijo McCormick, A., Unsicker, S.B., Gershenzon, J., 2012. The specificity of herbivore-induced plant volatiles in attracting herbivore enemies. Trends Plant Sci. 17, 303–310.
Dempsey, D.A., Klessig, D.F., 2017. How does the multifaceted plant hormone salicylic acid combat disease in plants and are similar mechanisms utilized in humans? BMC Biol. 15, 23.
Desurmont, G.A., Guiguet, A., Turlings, T.C., 2018. Invasive insect herbivores as disrupters of chemically-mediated tritrophic interactions: effects of herbivore density and parasitoid learning. Biol. Invasions 20, 195–206.
Duan, S.G., Li, D.Z., Wang, M.Q., 2019. Chemosensory proteins used as target for screening behaviourally active compounds in the rice pest cnaphalocrocis medinalis (Lepidoptera: Pyralidae). Insect Mol. Biol. 28, 123–135.
Erb, M., Robert, C.A., Hibbard, B.E., Turlings, T.C., 2011. Sequence of arrival determines plant-mediated interactions between herbivores. J. Ecol. 99, 7–15.
van Geem, M., Gols, R., Raaijmakers, C.E., Harvey, J.A., 2016. Effects of population-related variation in plant primary and secondary metabolites on aboveground and belowground multitrophic interactions. Chemoecology 26, 219–233.
Gorb, E.V., Gorb, S.N., 2017. Anti-adhesive effects of plant wax coverage on insect attachment. J. Exp. Bot. 68, 5323–5337.
Guo, H., Ge, F., 2017. Root nematode infection enhances leaf defense against whitefly in tomato. ArthropodPlant Interact. 11, 23–33.
Hakes, A.S., Cronin, J.T., 2012. Successional changes in plant resistance and tolerance to herbivory. Ecology 93, 1059–1070.
Herve, M.R., Erb, M., 2019. Distinct defense strategies allow different grassland species to cope with root herbivore attack. Oecologia 191, 127–139.
Hol, W.G., De Boer, W., Termorshuizen, A.J., Meyer, K.M., Schneider, J.H., Van Der Putten, W.H., Van Dam, N.M., 2013. Heterodera schachtii nematodes interfere with aphid-plant relations on brassica oleracea. J. Chem. Ecol. 39, 1193–1203.
Hoysted, G.A., Bell, C.A., Lilley, C.J., Urwin, P.E., 2018. Aphid colonization affects potato root exudate composition and the hatching of a soil borne pathogen. Front. Plant Sci. 9, 1278.
Huot, B., Yao, J., Montgomery, B.L., He, S.Y., 2014. Growth-defense tradeoffs in plants: a balancing act to optimize fitness. Mol. Plant 7, 1267–1287.
Hussain, M., Debnath, B., Qasim, M., Bamisile, B.S., Islam, W., Hameed, M.S., Wang, L., Qiu, D., 2019. Role of saponins in plant defense against specialist herbivores. Molecules 24, 2067.
Jang, G., Yoon, Y., Choi, Y.D., 2020. Crosstalk with jasmonic acid integrates multiple responses in plant development. Int. J. Mol. Sci. 21, 305.
Johnson, S.N., Young, M.W., Karley, A.J., 2012. Protected raspberry production alters aphid-plant interactions but not aphid population size. Agric. For. Entomol. 14, 217–224.
Kafle, D., Hänel, A., Lortzing, T., Steppuhn, A., Wurst, S., 2017. Sequential above-and belowground herbivory modifies plant responses depending on herbivore identity. BMC Ecol. 17, 1–10.
Kant, M.R., Jonckheere, W., Knegt, B., Lemos, F., Liu, J., Schimmel, B.C., Villarroel, C.A., Ataide, L.M., Dermauw, W., Glas, J.J., Egas, M., Janssen, A., Van Leeuwen, T., Schuurink, R.C., Sabelis, M.W., Alba, J.M., 2015. Mechanisms and ecological consequences of plant defence induction and suppression in herbivore communities. Ann. Bot. 115, 1015–1051.
Karley, A.J., Mitchell, C., Brookes, C., McNicol, J., O'Neill, T., Roberts, H., Graham, J., Johnson, S.N., 2016. Exploiting physical defence traits for crop protection: leaf trichomes of rubus idaeushave deterrent effects on spider mites but not aphids. Ann. Appl. Biol. 168, 159–172.
Karssemeijer, P.N., Reichelt, M., Gershenzon, J., van Loon, J., Dicke, M., 2020. Foliar herbivory by caterpillars and aphids differentially affects phytohormonal signalling in roots and plant defence to a root herbivore. Plant Cell Environ. 43, 775–786.
Kastner, J., von Knorre, D., Himanshu, H., Erb, M., Baldwin, I.T., Meldau, S., 2014. Salicylic acid, a plant defense hormone, is specifically secreted by a molluscan herbivore. PLoS One 9, e86500.
Klessig, D.F., Choi, H.W., Dempsey, D.A., 2018. Systemic acquired resistance and salicylic acid: past, present, and future. Mol. Plant-Microbe Interact. 31, 871–888.
Koch, K.G., Chapman, K., Louis, J., Heng-Moss, T., Sarath, G., 2016. Plant tolerance: a unique approach to control hemipteran pests. Front. Plant Sci. 7, 1363.
Koornneef, A., Leon-Reyes, A., Ritsema, T., Verhage, A., Den Otter, F.C., Van Loon, L., Pieterse, C.M., 2008. Kinetics of salicylate-mediated suppression of jasmonate signaling reveal a role for redox modulation. Plant Physiol. 147, 1358–1368.
Ku, Y.S., Sintaha, M., Cheung, M.Y., Lam, H.M., 2018. Plant hormone signaling crosstalks between biotic and abiotic stress responses. Int. J. Mol. Sci. 19, 3206.
Kusnierczyk, A., Tran, D.H.T., Winge, P., Jorstad, T.S., Reese, J.C., Troczynska, J., Bones, A.M., 2011. Testing the importance of jasmonate signalling in induction of plant defences upon cabbage aphid (Brevicoryne brassicae) attack. BMC Genomics 12, 1–16.
Langridge, P., 2013. Wheat genomics and the ambitious targets for future wheat production. Genome 56, 545–547.
Liu, Q., Li, S., Ding, W., 2020. Aphid-induced tobacco resistance against ralstonia solanacearum is associated with changes in the salicylic acid level and rhizospheric microbial community. Eur. J. Plant Pathol. 157, 465–483.
Loake, G., Grant, M., 2007. Salicylic acid in plant defence-the players and protagonists. Curr. Opin. Plant Biol. 10, 466–472.
Louis, J., Basu, S., Varsani, S., Castano-Duque, L., Jiang, V., Williams, W.P., Felton, G.W., Luthe, D.S., 2015. Ethylene contributes to maize insect resistance1-mediated maize defense against the phloem sap-sucking corn leaf aphid. Plant Physiol. 169, 313–324.
Mbaluto, C.M., Ahmad, E.M., Madicke, A., Grosser, K., van Dam, N.M., Martinez-Medina, A., 2021. Induced local and systemic defense responses in tomato underlying interactions between the root-knot nematode Meloidogyne incognita and the potato aphid Macrosiphum euphorbiae. Front. Plant Sci. 12, 632212.
Mitchell, C., Brennan, R.M., Graham, J., Karley, A.J., 2016. Plant defense against herbivorous pests: exploiting resistance and tolerance traits for sustainable crop protection. Front. Plant Sci. 7, 1132.
Molero, G., Reynolds, M.P., 2020. Spike photosynthesis measured at high throughput indicates genetic variation independent of flag leaf photosynthesis. Field Crops. Res. 255, 107866.
Molinari, S., Loffredo, E., 2006. The role of salicylic acid in defense response of tomato to root-knot nematodes. Physiol. Mol. Plant Pathol. 68, 69–78.
Morkunas, I., Mai, V., Gabrys, B., 2011. Phytohormonal signaling in plant responses to aphid feeding. Acta Physiol. Plant. 33, 2057–2073.
Mur, L.A., Kenton, P., Atzorn, R., Miersch, O., Wasternack, C., 2006. The outcomes of concentration-specific interactions between salicylate and jasmonate signaling include synergy, antagonism, and oxidative stress leading to cell death. Plant Physiol. 140, 249–262.
Nalam, V., Louis, J., Shah, J., 2019. Plant defense against aphids, the pest extraordinaire. Plant Sci. 279, 96–107.
Pan, X., Welti, R., Wang, X., 2010. Quantitative analysis of major plant hormones in crude plant extracts by high-performance liquid chromatography-mass spectrometry. Nat. Protoc. 5, 986–992.
Paré, P.W., Tumlinson, J.H., 1999. Plant volatiles as a defense against insect herbivores. Plant Physiol. 121, 325–331.
Pierre, P.S., Dugravot, S., Ferry, A., Soler, R., van Dam, N.M., Cortesero, A.M., 2011. Aboveground herbivory affects indirect defences of brassicaceous plants against the root feeder Delia radicum Linnaeus: laboratory and field evidence. Ecol. Entomol. 36, 326–334.
Pieterse, C.M., Leon-Reyes, A., Van der Ent, S., Van Wees, S.C., 2009. Networking by small-molecule hormones in plant immunity. Nat. Chem. Biol. 5, 308–316.
Rasmann, S., Turlings, T.C., 2007. Simultaneous feeding by aboveground and belowground herbivores attenuates plant-mediated attraction of their respective natural enemies. Ecol. Lett. 10, 926–936.
Robert, C.A., Ferrieri, R.A., Schirmer, S., Babst, B.A., Schueller, M.J., Machado, R.A., Arce, C.C., Hibbard, B.E., Gershenzon, J., Turlings, T.C., Erb, M., 2014. Induced carbon reallocation and compensatory growth as root herbivore tolerance mechanisms. Plant Cell Environ. 37, 2613–2622.
Schweiger, R., Heise, A.M., Persicke, M., Muller, C., 2014. Interactions between the jasmonic and salicylic acid pathway modulate the plant metabolome and affect herbivores of different feeding types. Plant Cell Environ. 37, 1574–1585.
Shi, J.H., Sun, Z., Hu, X.J., Jin, H., Foba, C.N., Liu, H., Wang, C., Liu, L., Li, F.F., Wang, M.Q., 2019. Rice defense responses are induced upon leaf rolling by an insect herbivore. BMC Plant Biol. 19, 514.
Soler, R., Bezemer, T.M., Cortesero, A.M., Van der Putten, W.H., Vet, L.E., Harvey, J.A., 2007a. Impact of foliar herbivory on the development of a root-feeding insect and its parasitoid. Oecologia 152, 257–264.
Soler, R., Harvey, J.A., Kamp, A.F.D., Vet, L.E.M., Putten, W.H.V.D., Dam, N.M.V., Stuefer, J.F., Gols, R., Hordijk, C.A., Bezemer, T.M., 2007. Root herbivores influence the

behaviour of an aboveground parasitoid through changes in plant-volatile signals. Oikos 116, 367–376.
Sun, Z., Liu, Z., Zhou, W., Jin, H., Liu, H., Zhou, A., Zhang, A., Wang, M.Q., 2016. Temporal interactions of plant - insect - predator after infection of bacterial pathogen on rice plants. Sci. Rep. 6, 26043.
Team, R.C., 2013. R: A language and environment for statistical computing.
Tsunoda, T., Grosser, K., van Dam, N.M., 2018. Locally and systemically induced glucosinolates follow optimal defence allocation theory upon root herbivory. Funct. Ecol. 32, 2127–2137.
Turlings, T.C.J., Erb, M., 2018. Tritrophic interactions mediated by herbivore-induced plant volatiles: mechanisms, ecological relevance, and application potential. Annu. Rev. Entomol. 63, 433–452.
Underwood, N., 2000. Density dependence in induced plant resistance to herbivore damage: threshold, strength and genetic variation. Oikos 89, 295–300.
Verberne, M.C., Hoekstra, J., Bol, J.F., Linthorst, H.J., 2003. Signaling of systemic acquired resistance in tobacco depends on ethylene perception. Plant J. 35, 27–32.
Verma, V., Ravindran, P., Kumar, P.P., 2016. Plant hormone-mediated regulation of stress responses. BMC Plant Biol. 16, 1–10.
Wäckers, F.L., Bezemer, T.M., 2003. Root herbivory induces an above-ground indirect defence. Ecol. Lett. 6, 9–12.
Wasternack, C., Hause, B., 2013. Jasmonates: biosynthesis, perception, signal transduction and action in plant stress response, growth and development. An update to the 2007 review in annals of botany. Ann. Bot. 111, 1021–1058.
Wei, J., van Loon, J.J., Gols, R., Menzel, T.R., Li, N., Kang, L., Dicke, M., 2014. Reciprocal crosstalk between jasmonate and salicylate defence-signalling pathways modulates plant volatile emission and herbivore host-selection behaviour. J. Exp. Bot. 65, 3289–3298.
Will, T., Tjallingii, W.F., Thonnessen, A., van Bel, A.J., 2007. Molecular sabotage of plant defense by aphid saliva. Proc. Natl. Acad. Sci. U. S. A. 104, 10536–10541.
Xu, J., Wang, X., Zu, H., Zeng, X., Baldwin, I.T., Lou, Y., Li, R., 2021. Molecular dissection of rice phytohormone signaling involved in resistance to a piercing-sucking herbivore. New Phytol. 230, 1639–1652.
Yang, H., Wang, Y., Li, L., Li, F., He, Y., Wu, J., Wei, C., 2019. Transcriptomic and phytochemical analyses reveal root-mediated resource-based defense response to leaf herbivory by ectropis oblique in tea plant (Camellia sinensis). J. Agric. Food Chem. 67, 5465–5476.
Yuan, M., Huang, Y., Ge, W., Jia, Z., Song, S., Zhang, L., Huang, Y., 2019. Involvement of jasmonic acid, ethylene and salicylic acid signaling pathways behind the systemic resistance induced by Trichoderma longibrachiatum H9 in cucumber. BMC Genomics 20, 144.
Zhang, P.J., Broekgaarden, C., Zheng, S.J., Snoeren, T.A., van Loon, J.J., Gols, R., Dicke, M., 2013. Jasmonate and ethylene signaling mediate whitefly-induced interference with indirect plant defense in Arabidopsis thaliana. New Phytol. 197, 1291–1299.
Zhao, W., Li, Z., Fan, J., Hu, C., Yang, R., Qi, X., Chen, H., Zhao, F., Wang, S., 2015. Identification of jasmonic acid-associated microRNAs and characterization of the regulatory roles of the miR319/TCP4 module under root-knot nematode stress in tomato. J. Exp. Bot. 66, 4653–4667.
Zust, T., Agrawal, A.A., 2017. Trade-offs between plant growth and defense against insect herbivory: an emerging mechanistic synthesis. Annu. Rev. Plant Biol. 68, 513–534.